and study its properties as a funcion of the coefficients $\xi$ and $\chi$. In general, the solutions can be obtained numerically by diagonalizing the Hamiltonian. In this contribution, we employ the large $N$ limit in which approximate solutions can be obtained in closed form and which may help to achieve a better understanding of the basic features of the model.

The large $N$ (or classical) limit of the IBM Hamiltonian can be studied by introducing a coherent (or intrinsic) state which has the form of a boson condensate, a superposition of monopole and quadrupole bosons [4, 5]

$$\begin{aligned} |g\rangle &= \frac{1}{\sqrt{N!}}\left(b_c^\dagger\right)|0\rangle\,, \\ b_c^\dagger &= \frac{1}{\sqrt{1+\beta^2}}\left[s^\dagger + \beta\left(d_0^\dagger\cos\gamma + \frac{1}{\sqrt{2}}(d_2^\dagger + d_{-2}^\dagger)\sin\gamma\right)\right]. \end{aligned} \tag{2}$$

Here $\beta$ and $\gamma$ denote the deformation parameters in the IBM. The associated energy surface is obtained as the expectation value of the (normal ordered) Hamiltonian in the intrinsic state

$$\frac{1}{N}E(\beta,\gamma) = \frac{1}{N}\langle g|:H:|g\rangle = (1-\xi)\frac{\beta^2}{1+\beta^2} - \xi\frac{\frac{2}{7}\chi^2\beta^4 - 4\sqrt{\frac{2}{7}}\chi\beta^3\cos 3\gamma + 4\beta^2}{4(1+\beta^2)^2}\,. \tag{3}$$

The equilibrium shape is defined as the minimum in the energy surface and is characterized by $\beta_0$, $\gamma_0$. Quantum phase transitions can be studied by varying the control parameter $\xi$ over the range $0 \le \xi \le 1$ [4].

For $\chi = 0$, the Hamiltonian exhibits a second-order phase transition between the $U(5)$ and $SO(6)$ limits separated by the critical point $\xi_c = \frac{1}{2}$. For $0 \le \xi < \xi_c$ the equilibrium shape is spherical ($\beta_0 = 0$) and for $\xi_c < \xi \le 1$ it is deformed ($\beta_0 > 0$).

For $\chi = \mp\sqrt{7}/2$, the Hamiltonian exhibits a first-order phase transition between the $U(5)$ and $SU(3)$ limits separated by the critical point $\xi_c = \frac{8}{17}$. For $0 \le \xi < \xi_c$ the equilibrium shape is spherical ($\beta_0 = 0$) and for $\xi_c < \xi \le 1$ it is axially deformed ($\beta_0 > 0$) with prolate symmetry for $\chi = -\sqrt{7}/2$ and oblate symmetry for $\chi = +\sqrt{7}/2$.

In the general case, for $0 < |\chi| \le \sqrt{7}/2$ one has a first-order phase transition between the spherical and deformed phase. For $\xi < \xi_c$ the equilibrium shape is spherical ($\beta_0 = 0$), and for $\xi > \xi_c$ the equilibrium shape is deformed ($\beta_0 > 0$) with prolate symmetry for $\chi < 0$ ($\gamma_0 = 0°$) and oblate symmetry for $\chi > 0$ ($\gamma_0 = 180°$). Here, the $z$-axis is chosen along the symmetry axis.

For the case of a pure quadrupole-quadrupole interaction ($\xi = 1$) the equilibrium value of the deformation parameter is given by [6]

$$\beta_0 = \frac{1}{2}\left(\sqrt{\frac{2}{7}}|\chi| + \sqrt{\frac{2}{7}\chi^2 + 4}\right), \tag{4}$$

which increases from the $SO(6)$ value $\beta_0 = 1$ for $\chi = 0$ to the $SU(3)$ value $\beta = \sqrt{2}$ for $|\chi| = \sqrt{7}/2$.

Fig. 1 shows the equilibrium value of the deformation parameter as a function of the control parameter, $\xi$, and the structure of the quadrupole operator, $\chi$.

Excited bands arise as intrinsic excitations of the ground state band

$$\begin{aligned} |\beta\rangle &= \frac{1}{\sqrt{N}}\,b_\beta^\dagger b_c|g\rangle\,, & b_\beta^\dagger &= \frac{1}{\sqrt{1+\beta^2}}\left(-\beta s^\dagger + d_0^\dagger\right), \\ |\gamma\rangle &= \frac{1}{\sqrt{N}}\,b_\gamma^\dagger b_c|g\rangle\,, & b_\gamma^\dagger &= \frac{1}{\sqrt{2}}\left(d_2^\dagger + d_{-2}^\dagger\right). \end{aligned} \tag{5}$$

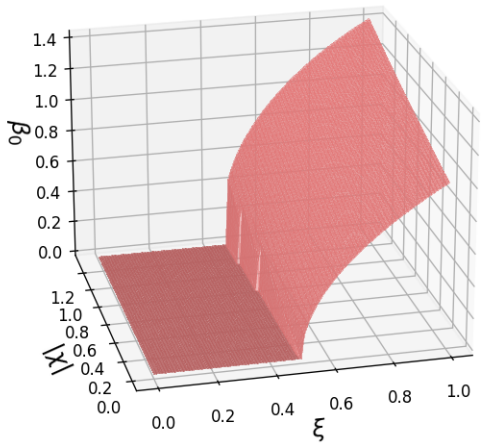


**Figure 1.** Equilibrium value of the deformation parameter $\beta$.

The intrinsic energies of the $\beta$- and $\gamma$-band can be obtained in the large $N$ limit [7]. The ratio

$$E_{\gamma\beta} = \frac{E_\gamma}{E_\beta} = \frac{9\sqrt{\frac{2}{7}}|\chi|\beta_0}{4+\sqrt{\frac{2}{7}}|\chi|\beta_0(\beta_0^2+3)}\,, \tag{6}$$

does not depend explicitly on the control parameter $\xi$, but implicitly it does through the determination of the equilibrium value of the deformation parameter $\beta_0$ for each combination of $\xi$ and $\chi$.

In the consistent Q-formalism, the same quadrupole operator is used for the Hamiltonian and the $E2$ transition operator [8]. The ratio of intrinsic transition rates depends on the intrinsic matrix elements for the transitions between the ground state band and the $\beta$- and $\gamma$-band [9]

$$R_{\beta\gamma} = \frac{|\langle\beta|T_0(E2)|g\rangle|^2}{|\langle\gamma|T_2(E2)+T_{-2}(E2)|g\rangle|^2} = \frac{1}{2(1+\beta_0^2)}\left(\frac{1+\sqrt{\frac{2}{7}}|\chi|\beta_0-\beta_0^2}{1-\sqrt{\frac{2}{7}}|\chi|\beta_0}\right)^2\,. \tag{7}$$

Fig. 2 shows the relative intrinsic energies and transition probabilities for the deformed region $\xi_c < \xi < 1$ and $0 \le |\chi| \le \sqrt{7}/2$. For a given value of $\chi$, the ratio of intrinsic energies $E_{\gamma\beta}$ increases with $\xi$. In the $SU(3)$ limit ($\chi = \mp\sqrt{7}/2$ and $\xi = 1$) the intrinsic energies of the $\beta$- and $\gamma$-band are the same, whereas in the rest of the parameter space in the $\xi\chi$-plane the ratio $E_{\gamma\beta} < 1$.

For the large majority of the parameter space the behavior of the intrinsic transition rates is the opposite: for a given value of $\chi$, the ratio of intrinsic energies $R_{\beta\gamma}$ decreases with $\xi$ until it vanishes for the case of a pure quadrupole-quadrupole interaction ($\xi = 1$). Only for values $1 < |\chi| < \sqrt{7}/2$ the ratio first increases before decreasing to 0. For the $SU(3)$ value $|\chi| = \sqrt{7}/2$ the ratio of intrinsic transition rates continues to increase with $\xi$ to reach the value of $R_{\beta\gamma} = 3/2$ in the exact $SU(3)$ limit. The general trend is that for the larger part of

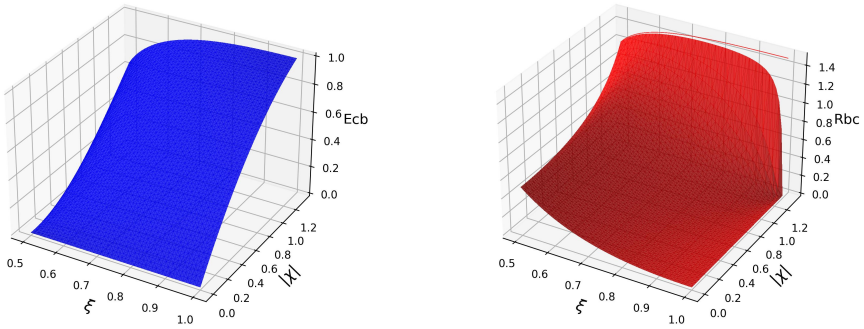


**Figure 2.** Ratio of intrinsic energies $E_\gamma/E_\beta$ (left) and intrinsic transition probabilities $R^2_\beta/R^2_\gamma$ (right).

the parameter space $g \to \gamma$ transitions are stronger than $g \to \beta$ transitions. Only when $\chi$ is getting close to the $SU(3)$ value of $\mp\sqrt{7}/2$ the two transitions become comparable, and the $g \to \beta$ transitions may even become stronger than the $g \to \gamma$ transitions.

At this stage it is important to emphasize that the results for the intrinsic energies and the quadrupole transitions are based on the large $N$ limit of the IBM in which the coupling between rotations and vibrations is neglected.

## 3 Case studies

As an illustration we apply the above analysis in the intrinsic IBM to three deformed nuclei, $^{156}$Gd, $^{162}$Dy and $^{168}$Er. These nuclei have a $R_{42} = E_{\rm exc}(4^+_1)/E_{\rm exc}(2^+_1)$ ratio of 3.24, 3.29 and 3.31, respectively, all very close to the rotational value of 10/3. The intrinsic energies are determined by subtracting the rotational contribution to the experimental energies: $E_\beta = E_{0^+_\beta}$ and $E_\gamma = E_{2^+_\gamma} - 6/2\mathcal{I}_\gamma$ where $\mathcal{I}_\gamma$ is the moment of inertia of the $\gamma$-band. The intrinsic transition rates can be determined from the ratio of $B(E2)$ values

$$R_{\beta\gamma} = \frac{B(E2; 0^+_g \to 2^+_\beta)}{B(E2; 0^+_g \to 2^+_\gamma)} \,. \tag{8}$$

The results are summarized in Table 1.

The nucleus $^{168}$Er has been the subject of an extensive study in IBM-1 in terms of a mixture of the $SU(3)$ and the $SO(6)$ quadrupole-quadrupole interactions [14] which in the present analysis effectively translates into a smaller (absolute) value of $\chi$. The value of the

**Table 1.** Ratio of intrinsic energies and transitions. The theoretical values are calculated according to Eqs. (6) and (7). The experimental values are taken from [10–13].

| | | | | Intrinsic IBM | | Experiment | |
|---|---|---|---|---|---|---|---|
| Nucleus | $R_{42}$ | $\xi$ | $\chi$ | $E_{\gamma\beta}$ | $R_{\beta\gamma}$ | $E_{\gamma\beta}$ | $R_{\beta\gamma}$ |
| $^{156}$Gd | 3.24 | 0.98 | −1.29 | 0.998 | 0.131 | 1.019 | $0.135 \pm 0.009$ |
| $^{162}$Dy | 3.29 | 0.84 | −0.65 | 0.584 | 0.063 | 0.581 | $0.063^{+0.024}_{-0.063}$ |
| $^{168}$Er | 3.31 | 0.93 | −0.64 | 0.611 | 0.012 | 0.613 | $0.012 \pm 0.002$ |

control parameter $\xi$ is close to that for a pure quadrupole-quadrupole interaction, $\xi = 0.93$ and the structure of the quadrupole operator is given by $\chi = -0.64$. Fig. 3 shows that there is only a very small region in the parameter space of the $\xi\chi$-plane where both the ratio of intrinsic energies (green) and transitions (blue) can be reproduced. The properties of $^{168}$Er have also been analyzed in the framework of partial dynamical symmetries of the IBM [15].

The nucleus $^{156}$Gd is usually presented as the standard example of a nucleus with $SU(3)$ symmetry with almost degenerate $\beta$- and $\gamma$-bands [5]. We find a good description of the ratio of intrinsic energies and transition rates for $\xi = 0.98$ and $\chi = -1.29$. Just as for $^{168}$Er there is only a very small range in the $\xi\chi$-plane that can reproduce the experimental values. It is important to note that the robust prediction made in Ref. [16] of very small values of $R_{\beta\gamma}$ only holds for a pure quadrupole-quadrupole interaction, $\xi = 1$ and $\chi \neq \mp\sqrt{7}/2$. In this case the intrinsic matrix element for $\beta \rightarrow g$ transitions vanishes in the large $N$ limit. Inspection of Fig. 2 shows that a small breaking of the $SU(3)$ limit, $\xi = 0.98$ and $\chi = -1.29$, makes it possible to reproduce the experimental value $R_{\beta\gamma} = 0.13$.

The final example is that of the nucleus $^{162}$Dy. This analysis is based partially on as of yet unpublished data on lifetime measurements. In [12] it was concluded that the first excited $K^P = 0^+$ band at 1400.2 keV is a genuine $\beta$-vibration. The ratio of intrinsic transion rates was extracted from the quadrupole transitions of the $2^+_\gamma$ state at 888 keV and the $2^+_\beta$ state at 1453 keV to the ground state band [13]

$$\begin{aligned} B(E2; 2^+_\gamma \rightarrow 0^+_g) &= 4.68 \pm 0.21 \text{ WU} \\ B(E2; 2^+_\beta \rightarrow 4^+_g) &= 0.76^{+0.29}_{-0.76} \text{ WU} \end{aligned} \tag{9}$$

In this case, the area of allowed values in the $\xi\chi$-plane is a bit larger because of the experimental uncertainty in the $2^+_\beta \rightarrow 4^+_g$ transition, especially in the $\xi$ direction.

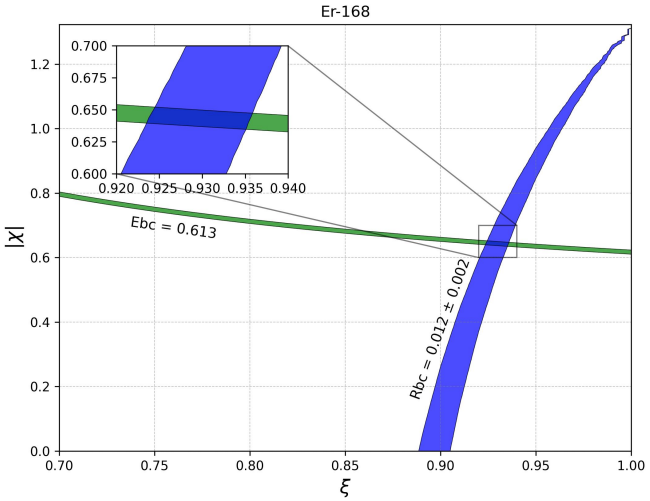


**Figure 3.** Ratio of intrinsic energies and quadrupole transitions in $^{168}$Er.